943

Pergamon

Carbon, Vol. 32, No. 6, pp. 1171–1176, 1994

0008-6223/94 $6.00 + .00

0008-6223(94)00080-8

ACTIVATION OF ANTHRACITE: USING CARBON DIOXIDE VERSUS AIR

G. A. R. BESSANT and P. L. WALKER, JR.
Department of Materials Science and Engineering, The Pennsylvania State University, University Park, PA 16802, U.S.A.

(*Received* 11 *March* 1994; *accepted* 6 *May* 1994)

Abstract—Devolatilized (950°C) anthracite was activated in 0.1 MPa CO_2 at 950°C and 0.1 MPa air at 425°C and 450°C. At comparable gasification rates and carbon burn-offs in CO_2 and air, larger surface areas and pore volumes were developed by activation in CO_2. This is attributed foremost to less uniform activation through the anthracite particles when gasification takes place in air. Also, the formation of a stable oxygen complex, concurrent with carbon gasification in air, may reduce the efficiency of anthracite activation.

Key Words—Anthracite, activation, carbon dioxide, air gasification.

1. INTRODUCTION

Anthracite has a considerable porosity, with a large fraction of the porosity in pore sizes of molecular dimensions[1–12]. Suitably treated, this fine pore structure in anthracite can be utilized for the successful production of activated carbon. Treatment involves selective removal of carbon atoms by gasification, resulting in both the opening up of pores closed to He and the enlargement of existing open porosity. To achieve optimum activation upon carbon gasification, it is important that gasification occurs essentially uniformly (in the radial direction) through the anthracite particles. This occurs when the concentration of reacting (activating) gas decreases little from the exterior to the center of the particle during gasification, or when the resistance to diffusion of the activating gas through the particle is small compared to the chemical resistance to gasification. This is denoted as Zone I kinetics[13]. At the other extreme, when resistance to diffusion is very large compared to resistance to gasification, carbon removal occurs solely at the exterior of the particle, and no activation of the remainder of the particle occurs. This is denoted as Zone III kinetics[13].

Since raw and devolatilized anthracites contain little transitional or macropore volume (or feeder pores) compared to micropore volume, resistance to diffusion of the activating gas through the particle will be relatively high. Hence, anthracite will be quite susceptible to non-uniform carbon gasification during the activation process. In this paper, the success of anthracite activation (as measured by increases in surface area and pore volume) will be followed using CO_2 versus air as the activating medium. We will see that activation of anthracite in air is inferior to that in CO_2, because of the less favorable balance between the resistance to diffusion to that of chemical reactivity in the case of air.

2. EXPERIMENTAL

2.1 *Anthracite used*

Anthracite from the Trevorton, Pennsylvania breaker of the Reading Anthracite Company was used for all activation runs reported in this study. Analysis of the 100 × 150 mesh (0.15 × 0.10 mm) size fraction (Tyler sieve series) is given in Table 1. This size fraction was used throughout the study.

2.2 *Activation of anthracite*

The activation apparatus is described in detail in previous papers[14,15]. Essentially, it consisted of a preheater, a fluidized bed reactor, and a product gas-analysis system. The fluidized reactor was a Hastelloy-C tube, 4.9 cm inside diameter by 153 cm in length. It was heated externally. The sample being activated was supported on a packed bed of 10 × 15 mesh alundum grains.

Experimental procedures are given in detail in previous papers[14,15]. The raw anthracite was first devolatilized in an N_2 stream at 950°C. The devolatilized anthracite was activated to the desired burn-off by monitoring the amounts of CO produced during reaction in CO_2, and CO and CO_2 produced during reaction in air. A part of the activated sample was set aside for study, and the remainder of the sample was used for subsequent runs at higher burn-off.

Prior to activation runs, the flow of reactant gas that should be used to obtain optimum fluidization conditions of anthracite was determined in a glass reactor of dimensions identical to the Hastelloy-C reactor. The preliminary study on fluidization is also described in detail in a previous paper[14]. In general, a good gas-solid contact and a uniform temperature distribution in the reactor are desirable characteristics of optimum fluidization conditions. However, the most important reason for employing a fluidized bed reac-

Table 1. Proximate analysis of raw anthracite

Moisture	0.8%
Volatile matter	9.1%
Ash	8.9%
Fixed carbon	81.2%

tor in this investigation was the desire to attain a uniform degree of activation of the anthracite particles throughout the entire bed. This condition is achieved when the fluidized bed shows an aggregative fluidized state. Under this condition, a good bottom to top turnover of solids may be achieved, resulting in a similar quality and extent of activation of each anthracite particle.

Activation was conducted at 950°C in 0.1 MPa of CO_2 and 425°C and 450°C in 0.1 MPa of air.

2.3 *Characterization of activated sample*

The activated anthracite samples were characterized by the following physical data: surface area from N_2 adsorption at −196°C using the BET equation, He density from He displacement, apparent density from Hg displacement, and total open pore volume. Nitrogen at −196°C is considered to be accessible to slit-shaped pores bounded by graphite-like basal planes greater than about 0.57 nm apart[16]. Mercury, at room temperature and 0.1 MPa pressure, is accessible to a negligible fraction of the total porosity in the anthracite samples.

3. RESULTS

For convenience, the activated anthracites were labeled as TRA (or TRC)-450-15, for example. T stands for Trevorton, the breaker from which the anthracite used for the activation studies was obtained, RA stands for reaction in air, RC stands for activation in CO_2, 450 is the activation temperature in degrees centigrade, and 15 stands for 15% burn-off of the starting devolatilized sample.

When correlating the experimental results, the ash content of the anthracite must be considered. It was assumed that during activation, (a) the ash was neither changed in chemical composition nor removed from the sample, and (b) the presence of ash did not contribute significantly to the development of internal porosity or surface area. The ash content of the devolatilized anthracite, 9.9%, is used as a basis for calculation. Percentages of burn-off on a dry, ash-free basis (d.a.f.), taking 90.1% of the devolatilized anthracite to be carbon, are calculated. Amounts of heteroatoms (H, O, N, and S) in the devolatilized anthracite are small. Unless otherwise stated, all correlations are based on a dry, ash-free basis.

3.1 *Gasification rates*

Figure 1 presents results for gasification rates in CO_2 at 950°C and air at 450°C and 425°C. Rates in CO_2 at 950°C and air at 450°C are essentially equal. In agreement with previous findings, gasification rates in air are much, much greater than gasification rates in CO_2 in Zones I and II[13] at the same temperatures and pressures.

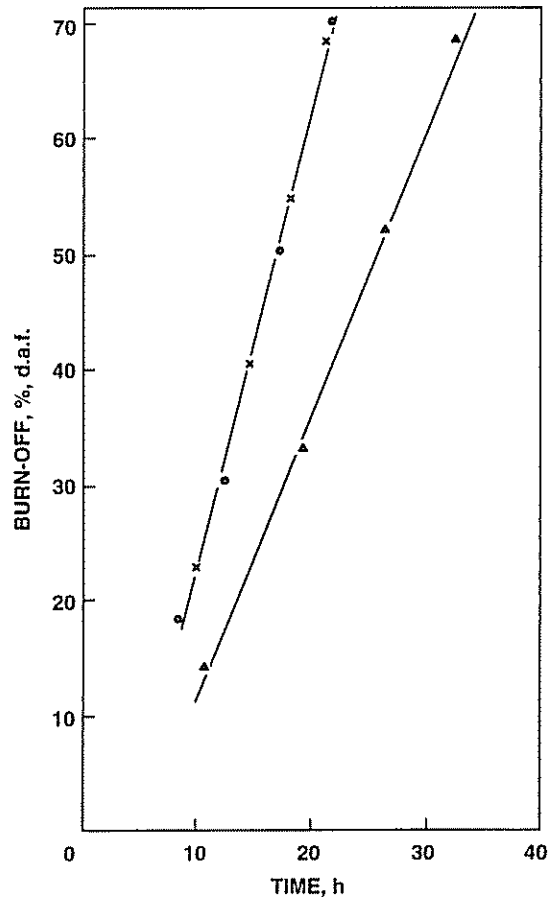

Fig. 1. Change in anthracite burn-off with time of activation in CO_2 at 950°C (●) and air at 425 (▲) and 450°C (×).

3.2 *Surface oxygen complex*

During carbon gasification in air at 425°C and 450°C, significant oxygen complex was formed on the carbon surface, which could not be removed at gasification temperature by outgassing following reaction. However, heating in N_2 at 850°C resulted in a significant decrease in sample weight as the oxygen complex was released as CO and CO_2. As seen in Fig. 2, the amount of complex increases with increasing duration of activation, but is independent of reaction temperature in the narrow temperature range 425°C–450°C. Assuming that the complex comes off as CO_2, 73%, by weight, of the complex is accounted for by oxygen. Heating subsequently to 950°C results in negligible additional weight loss, suggesting that the surface contains little additional complex. Outgassing the samples activated at 950°C in CO_2 at this temperature resulted in negligible weight loss. It is thought that little stable complex was formed during anthracite gasification in CO_2.

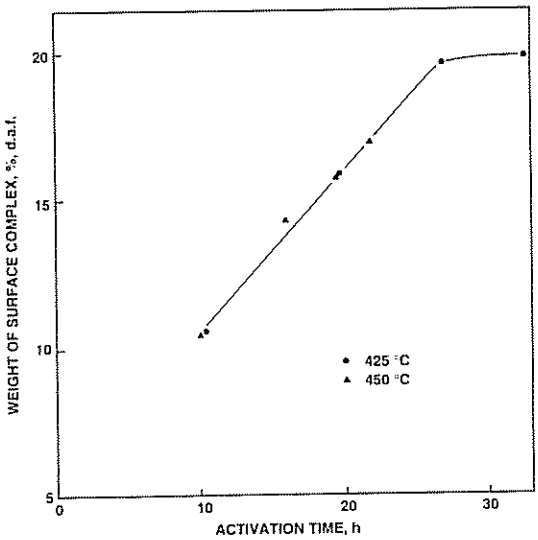

Fig. 2. Weight of surface complex formed during activation in air.

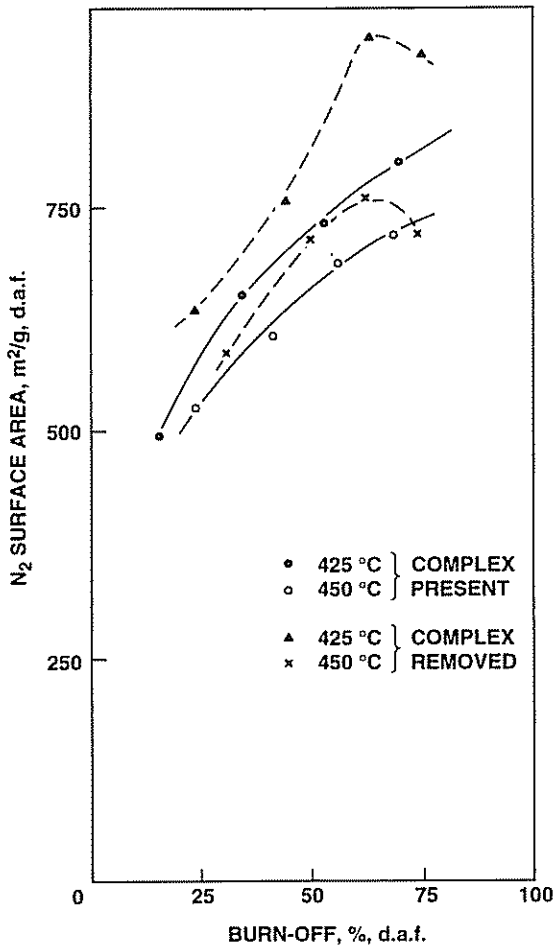

Fig. 3. Surface area developed by activation in air before and after removal of surface complex.

3.3 *Characterization of activated samples*

3.3.1 *Surface areas.* Table 2 summarizes results for surface areas of the samples following gasification in CO_2 and air to different burn-offs. For the samples activated in air, surface areas are also given following removal of surface complex at 850°C. Removal of complex results in additional carbon gasification and, consequently, significant further increases in surface area, as seen in Fig. 3. In any case, as seen in Fig. 4, activation in CO_2 at 950°C results in substantially higher surface areas than activation in air at either 425°C or 450°C.

3.3.2 *Densities and pore volumes.* After devolatilization at 950°C, anthracite may be considered to consist essentially of two phases, that is, the ash phase and the non-ash phase. If additivity of the volumes of the two phases is assumed[17], correction of the sample density for ash can be made using the following equation:

$$a/\gamma_a + (1 - a)/\gamma_c = 1/\gamma_m, \qquad (1)$$

where

γ_a = density of the ash;
γ_c = corrected density of the sample, d.a.f. basis;
γ_m = measured density of the sample, dry, ash containing basis;
a = weight fraction of ash present in the sample.

If it is assumed that a negligible internal porosity exists in the ash phase, the same value for the ash density can be used to correct the apparent and He densities. The He density of the devolatilized anthracite ash was measured to be 2.69 g/cc. Both the apparent and He densities on a d.a.f. basis for the non-ash phase are listed in Table 3. At equivalent burn-offs, it is seen that samples activated in CO_2 have smaller apparent densities and larger He densities than those activated in air.

Table 2. Surface areas for activated anthracite

Activation series	Burn-off, %, d.a.f.	Surface area, m^2/g, d.a.f	
TRC-950	16.5	505	
	27.7	800	
	45.8	1395	
	64.5	1825	
TRA-450	20.8	526	584[a]
	37.5	608	717
	50.0	690	760
	62.5	720	720
TRA-425	13.3	495	634
	30.3	654	758
	48.0	726	945
	63.0	813	920
Devolatilized anthracite	nil	12.2	

[a]Surface complex removed.

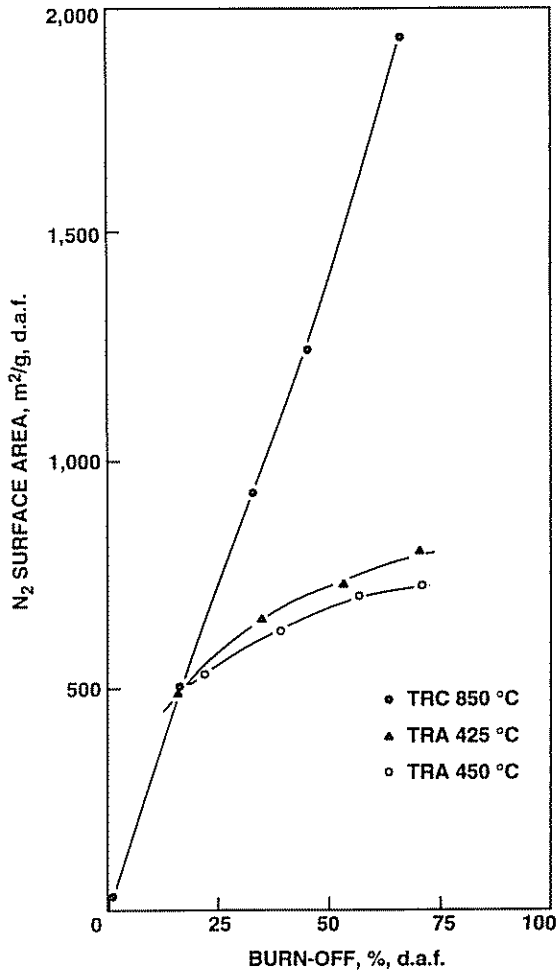

Fig. 4. Surface area developed by activation in CO_2 at 950°C and air.

Total pore volumes (given in Table 3) are calculated from differences between the apparent and He specific pore volumes using the following equation:

$$V_t = 1/\gamma_{app} - 1/\gamma_{He}, \quad (2)$$

where

γ_{app} = corrected apparent density of the sample d.a.f. basis;

γ_{He} = corrected He density of the sample, d.a.f. basis.

Helium is considered to be able to enter rapidly slit-like pores larger than 0.51 nm in width at room temperature[16]. Therefore, the total pore volume accessible to He (V_t) exists in pores or behind pore constrictions greater than 0.51 nm in width. It is seen, at higher burn-offs, that V_t developed from activation in CO_2 is considerably greater than that developed in air (Table 3).

Table 3. Densities and pore volumes for activated anthracite

Activated series	Burn-off d.a.f.	Densities, g/cc, d.a.f. Apparent	He	Pore volume cc/g, d.a.f.
TRC-950	16.5	1.40	2.05	0.226
	27.7	1.27	2.09	0.309
	45.8	1.05	2.15	0.487
	64.5	0.77	2.19	0.873
TRA-450	20.8	1.36	2.06	0.250
	37.5	1.17	2.07	0.379
	50.0	1.08	2.11	0.450
	62.5	0.98	2.11	0.544
TRA-425	13.3	1.45	2.02	0.195
	30.3	1.22	2.06	0.333
	48.0	1.04	2.05	0.472
	63.0	0.92	2.08	0.612
Raw anthracite	nil	1.49	1.60	0.046
Devolatilized anthracite	nil	1.62	1.96	0.106

4. DISCUSSION

A number of studies have been made on delineating the structure of anthracites using X-ray diffraction. Cartz and Hirsch conclude that an anthracite, having a fixed carbon content of about 90% (d.a.f.), consists primarily of graphite-like layers of about 0.75 nm average diameter[18]. In turn, on average, two layers are stacked in parallel. The anthracite also contains about 20% amorphous material (primarily carbon), which is thought to be crosslinks between the graphite-like bundles. The crosslinks prevent good alignment of the bundles and, hence, are responsible for the extensive microporosity found in anthracites.

When anthracite is heated to 950°C in N_2, volatile matter is released—primarily CO and CO_2 up to 750°C, and H_2 and CH_4 at higher temperatures[6]. Removal of carbon atoms during devolatilization results in counterbalancing effects. On the one hand, some removal results in opening up porosity previously inaccessible to He. On the other hand, removal of crosslinks results in achieving better alignment of the bundles, shrinkage of the anthracite particles, and loss of some porosity. The overall result from heating Trevorton anthracite to 950°C is an increase in He and apparent densities and in specific pore volumes.

Patel *et al.* [9] studied the effect of activating devolatilized anthracite in air at 425°C–430°C, followed by heating in N_2 at 950°C, on the accessibility of CH_4 into the structure. Following burn-off at 6.9%, CH_4 gained access to the micropores by activated diffusion, showing an activation energy of 28.0 kJ/mole. Additional activation to 8.0% burn-off resulted in a reduction in activation energy for diffusion to 11.7 kJ/mole. Further activation to 9.1% burn-off resulted in conversion of the diffusion coefficient for CH_4 access into the particle from activation diffusion to Knudsen diffusion. That is, over the temperature range of mea-

surements (25–70°C), a negligible activation energy was required for CH_4 access into the anthracite gasified to 9.1% burn-off. The diffusion coefficient varied with $T^{0.5}$, as was described by Knudsen diffusion[19].

For O_2, it is estimated that the critical pore dimension is 0.544 nm[16]. That is, just above this size, transport will be characterized by Knudsen diffusion. The Knudsen diffusion coefficient (D) is given by $D_K = (2r/3)(\bar{v})$ where r is the pore (void) radius and $\bar{v}$ is the average molecular velocity of O_2[19]. Just below this size (0.544 nm), diffusion will be characterized by activated diffusion, with the activation energy increasing very rapidly with decrease in void size, as given by the Lennard-Jones (6–12) potential function[20]. The critical dimension for CO_2 is estimated to be 0.542 nm[16].

Estimates can be made for values of diffusion coefficients for O_2 at 450°C and CO_2 at 950°C in devolatilized Trevorton anthracite based on previous studies of Walker and co-workers for diffusion of these gases from a carbon molecular sieve[21]. At 25°C the diffusion coefficients for O_2 and CO_2 were 6.8×10^{-9} cm^2/s and 2.3×10^{-9} cm^2/s, respectively[21]. Activation energies for the diffusion coefficients were 14 and 19 kJ/mole[21]. Extrapolation to 450°C yields a diffusion coefficient of 1.9×10^{-7} cm^2/s for O_2. Extrapolation to 950°C yields a diffusion coefficient of 7.4×10^{-7} cm^2/s for CO_2.

Estimates can also be made for values of diffusion coefficients for O_2 at 450°C and CO_2 at 950°C in Trevorton anthracite sufficiently activated to place diffusion of the gases in the Knudsen regime. The Knudsen regime will commence for both O_2 and CO_2 for a pore size slightly above 0.54 nm. Let us calculate D_K for a size of 0.60 nm at 25°C. D_K values for O_2 and CO_2 are 1.0×10^{-3} cm^2/s for O_2 and 0.82×10^{-3} cm^2/s for CO_2. Converting to reaction temperatures of 450°C for O_2 and 950°C for CO_2, D_K values are 1.5×10^{-3} cm^2/s and 1.7×10^{-3} cm^2/s.

Walker and co-workers discuss at length the criteria that can be used to determine what reaction zone one is in during carbon gasification (activation)[13]. The dimensionless group:

$$\beta = \left(\frac{Rn}{C_R D_{eff}}\right)\left(\frac{dw}{dt}\right) \tag{3}$$

can be used, where

n = 3 for a sphere;
R = particle radius;
C_R = concentration of the gaseous reactant at the outside surface of the particle;
D_{eff} = rate controlling diffusion coefficient through the particle;
dw/dt = diffusion rate of reactant (CO_2 or O_2) per unit of exterior surface area of the sample.

If β is less than about 0.1, the reaction is in Zone I, or gasification proceeds at essentially a uniform rate through the particle[13]. As β increases monotonically in value above 0.1, gasification becomes increasingly more non-uniform. That is, the diffusional resistance becomes increasingly more important in limiting (determining) the gasification rate.

The equal gasification rates in CO_2 at 950°C and air at 450°C, calculated from Fig. 1, can be converted to dw/dt, knowing how much reactant is consumed per mole of carbon gasified. For the C/CO_2 reaction, essentially one mole of CO_2 is consumed per mole of carbon gasified. For the C/air reaction at 450°C, the product CO_2/CO ratio was measured at essentially 3.1 at all levels of burn-off. Or 0.88 mole of O_2 was consumed per mole of carbon gasified.

First, let us estimate values for β for activation in O_2 at 450°C and CO_2 at 950°C at the beginning of gasification of the devolatilized Trevorton anthracite when activated diffusion is operative. Table 4 gives values for the parameters in eqn (3) needed to calculate β_{act}. It is seen that the β_{act}s are considerably above 0.1, and thus, in the beginning of gasification of the devolatilized anthracite, activation will be quite non-uniform through the particles. Further, it is seen that activation in air will be more non-uniform than activation in CO_2.

Patel and co-workers previously showed[9] that gasification to low burn-offs will quickly change activated diffusion to Knudsen diffusion with a dramatic increase in diffusion coefficient. Values of D_K previously calculated for O_2 at 450°C and CO_2 at 950°C were for a single pore 0.60 nm in width. The effective diffusion coefficient (D_{eff}) through the anthracite particles is, in turn, given by $D_{eff} = D_K\,(\theta/\tau)$ where θ is the particle porosity and τ is the tortuosity factor for travel within the particle[13,19]. The particle porosity is taken as 0.32, following 16.5% burn-off in CO_2 at 950°C. The appropriate value to take for τ is somewhat questionable; it increases sharply from about 1.4 to 80 as an artifact passes from an unconsolidated to a fully consolidated medium[19,22]. Hutcheon and co-workers found for a fine-pore graphite artifact that τ equalled about 20[23]. This value is used in this study for both CO_2 and air to calculate $D_{eff,K}$. Walker and co-workers have previously shown that τ decreases with increasing θ[13]; and, hence, it will decrease with increasing carbon

Table 4. Values of parameters in eqn (3)

	Conditions	
Parameters	Air, 450°C	CO_2, 950°C
R, cm	6.3×10^{-3}	6.3×10^{-3}
C_R, moles/cm^3	3.4×10^{-6}	1.0×10^{-5}
$D_{eff,act}$, cm^2/s	1.9×10^{-7}	7.4×10^{-7}
$D_{eff,K}$, cm^2/s	2.4×10^{-5}	2.7×10^{-5}
dw/dt, moles/s × cm^2	0.28×10^{-8}	0.32×10^{-8}
β_{act}	82	8.0
β_K	0.63	0.23

burn-off during anthracite activation. For these parameters, β_Ks are considerably less than β_{act}s for activation both in CO_2 and air, as seen in Table 4. But under these conditions, activation can still be expected to be somewhat non-uniform through the particles—with non-uniformity being greater for activation in air.

It is thus expected that development of surface area and pore volume during the activation in CO_2 at 950°C will be superior to development during activation in air at 450°C. Another fact that may contribute to poorer activation in air at 450°C is that activation at this low temperature results in the formation of considerable stable oxygen complex concurrent with carbon gasification. This chemisorbed oxygen could both block micropores previously opened up during gasification and also prevent reactant attack at some carbon sites, thus stopping the development of new porosity.

5. CONCLUSIONS

At comparable gasification rates in CO_2 and air, CO_2 is found to be a more efficient activating agent for a microporous carbon like anthracite. The greater efficiency of CO_2 is attributed to a more uniform activation through the particle at an equal gasification rate for CO_2 compared to air. The basic problem with air is its much higher intrinsic reactivity for carbon gasification compared to CO_2. If activation in air were to be conducted at the same temperature as for CO_2 (950°C, for example), the gasification rate in air would be much, much higher than that in CO_2. The result would be that the intrinsic resistance to carbon gasification in air would be small compared to the resistance to reactant O_2 diffusion into the porous particle. Thus, excessive gasification close to the exterior surface of the particle and little gasification close to the center would occur. Excessive non-uniform gasification in air can be reduced by lowering gasification temperature in air, as was done in this study. The problem appears to be that when the gasification temperature in air is reduced sufficiently to attain a gasification rate comparable to that occurring in CO_2, stable oxygen complex formation occurs concurrent with carbon gasification (and anthracite activation). The formation of the reactant complex appears to be deleterious to anthracite activation. Because carbon has a lower reactivity in CO_2, the activating temperature in CO_2 can be raised (for example, to 950°C); and at this temperature a negligible amount of stable oxygen complex is formed during carbon gasification.

REFERENCES

1. P. B. Hirsch, *Proc. Roy. Soc.* (London) **A226**, 143 (1954).
2. R. L. Bond and D. H. T. Spencer, *Proceedings First Industrial Carbon and Graphite Conference*, London, p. 231 (1958).
3. R. B. Anderson, W. K. Hall, J. A. Lecky, and K. C. Stein, *J. Phys. Chem.* **60**, 1548 (1956).
4. P. L. Walker, Jr. and I. Geller, *Nature* **178**, 1001 (1956).
5. J. L. Metcalfe, III, M. Kawahata, and P. L. Walker, Jr., *Fuel* **42**, 233 (1963).
6. S. P. Nandi, V. Ramadass, and P. L. Walker, Jr., *Carbon* **2**, 199 (1964).
7. P. L. Walker, Jr. and K. A. Kini, *Fuel* **44**, 453 (1965).
8. P. L. Walker, Jr. and R. L. Patel, *Fuel* **49**, 91 (1970).
9. R. L. Patel, S. P. Nandi, and P. L. Walker, Jr., *Fuel* **51**, 47 (1972).
10. H. Gan, S. P. Nandi, and P. L. Walker, Jr., *Fuel* **51**, 272 (1972).
11. P. L. Walker, Jr., *Phil. Trans. Roy. Soc.* (London) **A300**, 65 (1981).
12. P. L. Walker, Jr., S. K. Verma, J. Rivera-Utrilla, and A. Davis, *Fuel* **67**, 1615 (1988).
13. P. L. Walker, Jr., F. Rusinko, Jr., and L. G. Austin, In *Advances in Catalysis* (Edited by D. D. Eley, P. W. Selwood, and P. B. Weisz), Vol. 11, pp. 133–221. Academic Press, New York (1959).
14. M. Kawahata and P. L. Walker, Jr., *Proc. Anthracite Conf.*, Mineral Industries Experiment Station, The Pennsylvania State University, Bulletin No. 75, pp. 63–78 (1961).
15. M. Kawahata and P. L. Walker, Jr., *Proceedings Fifth Carbon Conference*, Vol. 2, pp. 251–263. Pergamon Press, Oxford (1963).
16. M. R. Rao, R. G. Jenkins, and W. A. Steele, *Langmuir* **1**, 137 (1985).
17. M. Kawahata, Ph.D. Thesis, The Pennsylvania State University, 1960.
18. L. Cartz and P. B. Hirsch, *Trans. Roy. Soc.* (London) **A252**, 557 (1960).
19. A. Wheeler, In *Advances in Catalysis* (Edited by W. G. Frankenburg, V. I. Komarewsky, and E. K. Rideal), Vol. 3, pp. 249–327. Academic Press, New York (1951).
20. P. L. Walker, Jr., L. G. Austin, and S. P. Nandi, In *Chemistry and Physics of Carbon* (Edited by P. L. Walker, Jr.), Vol. 2, pp. 257–371. Marcel Dekker, New York (1966).
21. P. L. Walker, Jr., *Carbon* **28**, 261 (1990).
22. M. R. Wyllie and W. D. Rose, *Trans. Amer. Inst. Min. Metall. Engrs.* **189**, 105 (1950).
23. J. M. Hutcheon, B. Longstaff, and R. K. Warner, *Proceedings First Industrial Carbon and Graphite Conference*, London, p. 259 (1958).